American Mineralogist, Volume 86, pages 115–123, 2001

Hydrothermal reactivity of Lu-saturated smectites: Part I. A long-range order study

M.D. ALBA, A.I. BECERRO, M.A. CASTRO,* AND A.C. PERDIGÓN

Departamento de Química Inorgánica, Instituto de Ciencia de Materiales, Universidad de Sevilla, Consejo Superior de Investigaciones Científicas, Avda. Américo Vespucio. 41092-Sevilla, Spain

ABSTRACT

Changes produced after hydrothermal treatments at 400 C and at different pressures in a set of Lu-saturated smectites have been compared with those occurring in a mixture of $2SiO_2$:$1Lu_2O_3$. The effect of the mineralogical composition of the smectite on the reactivity has been analyzed. The growth of a new crystalline phase, $Lu_2Si_2O_7$ (detected by means of X-ray diffraction), at a different pressure for each smectite, has allowed us to establish a reactivity order among the samples. All the samples were much more reactive than the mixture of oxides. The reactivity of the smectites was modulated by their different mineralogical compositions. First, smectites having Al in the tetrahedral sheet were the most reactive. This finding is interpreted as due to a strong electrostatic interaction created by the Al that activates neighboring Si for the reaction. Second, a higher reactivity was observed for the smectites with total occupancy of the octahedral sheet, due to the simultaneous disruption of the tetrahedral-octahedral shared oxygen layer and the diffusion of octahedral cations into the interlayer space. Third, the layer charge of the smectite does not induce any variation in the reactivity for the set of samples analyzed.

INTRODUCTION

Understanding the interaction mechanisms between the smectite lattice and the cations present in its interlayer space after thermal and hydrothermal treatments is important from both basic and applied points of view, and has attracted the attention of several research groups (Beall et al. 1979; Figueras 1988; Alvero et al. 1994). Within this general scheme, during the past decade our team has studied the possible mechanisms for the fixation of trivalent 4f cations that initially occupy exchangeable sites in the interlayer space of smectites (Trillo et al. 1990, 1992; Muñoz-Páez et al. 1994, 1995; Alba et al. 1996; Castro et al. 1996; Alba et al. 1997).

This systematic research has attempted to rationalize the behavior of the 4f series, considering the different geometrical structures and thermodynamic magnitudes, such as the Gibbs free-energies of formation, from a basic physicochemical point of view. We have also evaluated the ability of the smectites to immobilize the lanthanide ions (Ln^{3+}), a process of importance for the storage of radioactive wastes. For this latter purpose, Ln^{3+} ions are usually employed to mimic the actinide ones. We have reported the modifications shown by a montmorillonite exchanged with Lu^{3+} after hydrothermal treatment at 400 C (Trillo et al. 1994). The extensive formation of $Lu_2Si_2O_7$ after this treatment offers a possible and effective mechanism of radionuclide immobilization in high-level radioactive waste repositories. Such a possibility had not been considered previously due to the high temperatures reported in the phase diagrams for the systems SiO_2-Ln_2O_3 needed to yield lanthanide silicates (Felsche 1973).

It is important to know the structural properties of the smectites that enhance the reactivity of the Ln^{3+} ions leading to the formation of the disilicate phase. This information could be extremely useful in finding smectites that yield the disilicate phase under even milder conditions than those already reported, and would be especially relevant to the design of effective repositories for high-level radioactive wastes.

Our main aim in this paper is to characterize the formation of $Lu_2Si_2O_7$ from a set of different smectites saturated in Lu ions under hydrothermal conditions. These experiments reveal the effect of the chemical characteristics of the clay samples on the formation of $Lu_2Si_2O_7$. In addition, the hydrothermal treatment of the solid mixture of Lu_2O_3-SiO_2 has been studied and compared with the reactivity shown by the smectites. Thus, the differential reactivity of sheet and framework silicates for the formation of $Lu_2Si_2O_7$ has been determined.

Our study utilizes X-ray diffraction (XRD) techniques to characterize the modifications shown by a set of Lu-saturated smectites after several hydrothermal treatments at 400 C and different pressures. Differential thermal analysis (DTA) has been employed to study the effects of the hydrothermal reaction on the dehydration process of the residual smectite structure. Likewise, XRD on different types of oriented aggregates, together with chemical analyses of the exchangeable cations produced after the treatments, have been employed to determine the new composition of the interlayer space after the disappearance of the hydrated interlayer Lu ions.

* E-mail: mcastro@cica.es

EXPERIMENTAL METHODS

Materials

Starting smectites. We selected four well-characterized smectites for investigation and their structural formulae are listed in Table 1. The Trancos montmorillonite was supplied by Minas de Gádor (Almería), and the others were obtained from the Source Clay Minerals Repository, University of Missouri (Columbia). These smectites were selected to assess the influence of their mineralogical composition in the reaction studied. Figure 1 displays the location of each sample in a 3D graph showing the interlayer charge required to balance deficits in tetrahedral and octahedral sites (z-axis), the octahedral occupancies (y-axis), and the percentage of the layer charge generated by Al substituted for Si in the tetrahedral sites (x-axis). Regarding the layer charge deficit, all the samples are included in the 0.4-1.2 range of the smectite phyllosilicates, in agreement with the general recommendations of the international nomenclature committee (Association Internationale pour l'Etude des Argiles Nomenclature Committe 1980).

Exchanged smectites. Original smectite samples with particle diameters <2 m were used, after removal of carbonates and organic matter, as starting materials for the preparation of the Lu-saturated smectites by ion exchange according to the method described by Miller et al. (1982). High-purity Lu^{3+} nitrate was supplied by Strem Chemical Inc. (cat. no. 93-7113) to prepare the Lu solutions. Sodium-saturated smectites were used as reference materials, prepared in accordance with standard methods.

Oxide mixtures. SiO_2-Lu_2O_3 mixtures were employed to analyze the differential reactivity between the framework-lattice silicon oxides and the layer-lattice silicates in the formation of $Lu_2Si_2O_7$. A fine-grained silica powder (surface area ~ 200 m^2/g) and Lu_2O_3 were used, both of which were supplied by Sigma Chemical Co. (cat. nos. S5505 and L5126, respectively). Both oxides were gently mixed in an agate mortar. The proportions employed were $2SiO_2$:$1Lu_2O_3$; of the three compositional groups described in the Ln_2O_3:SiO_2 binary systems (Felsche 1973), this one is closest to that found in the Lu-saturated smectites.

Hydrothermal treatments

Hydrothermal treatments were carried out in Sno-Trik reactors consisting of pre-coned and tempered stainless-steel tubes closed at both ends with high-pressure caps. The powdered smectite sample and the amount of water necessary to reach the desired pressure were transferred into the reactors, which were heated at 400 C for 24 hours. This temperature was selected in accordance with our previous findings that extensive generation of $Lu_2Si_2O_7$ was attained in a reasonable reaction time of 24 hours. After the treatments, the samples were quenched, dried in air at 60 C, and ground in an agate mortar. The experimental variable was the pressure, which was selected according to the reactivity shown by the samples, using a range of 150 to 300 atm. The SiO_2-Lu_2O_3 mixture was reacted at 400 C and 250 atm for 24 hours.

Experimental techniques

X-ray powder diffraction. XRD patterns were obtained with a Siemens Kristalloflex D500 instrument, using Ni-filtered Cu$K\alpha$ radiation at 36 kV and 26 mA. Diffractograms were obtained from 3 to 70 2θ at a scanning speed of 0.05 2θ/min and with a counting time of 10 s. Background was subtracted from raw intensity data interactively using the computer program "Diffrac" in all the cases. XRD patterns of powdered samples were used to study the possible crystalline phases resulting from the hydrothermal treatments, as well as the modifications to the smectite lattice. The basal spacing resulting from the reaction for each sample was obtained from XRD patterns of aggregates oriented in water and in ethylene glycol (Moore

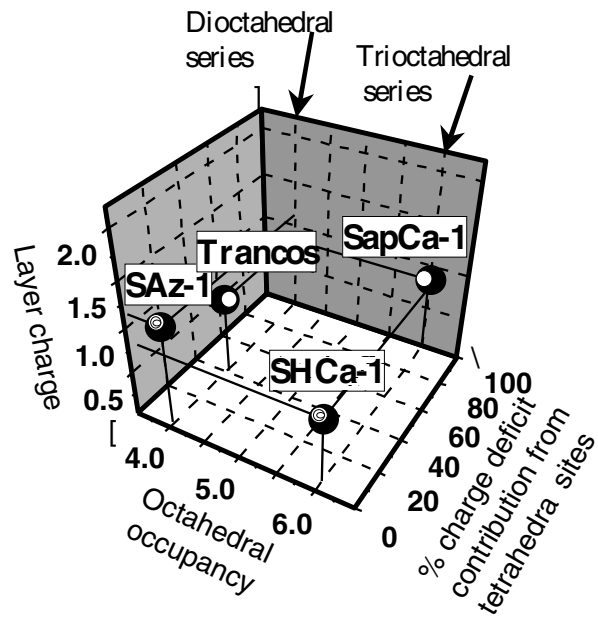

FIGURE 1. 3D graph representing the layer charge deficits, octahedral occupancies, and tetrahedral charge deficit contributions for the samples studied.

TABLE 1. Structural formulae of the selected smectites

Series	Short Name	$^{[4]}Si^{4+}$	$^{[4]}Al^{3+}$	$^{[6]}Al^{3+}$	$^{[6]}Fe^{3+}$	$^{[6]}Mg^{2+}$	$^{[6]}Li^{+}$	$^{[6]}Ti^{4+}$	M^{+}
Dioctahedral	Trancos*	7.64	0.36	3.09	0.28	0.69	–	–	0.87
	SAz-1†	7.97	0.03	2.71	0.14	1.13	–	0.02	1.14
Trioctahedral	SHCa-1‡	7.96	0.04	0.04	–	5.30	0.66	–	0.66
	SapCa-1§	7.20	7.20	0.80	0.14	5.79	–	–	0.80

* Montmorillonite; Trillo et al. (1990).
† Montmorillonite; Van Olphen and Fripiat (1979).
‡ Hectorite; Ames (1958).
§ Saponite; Becerro (1997).

and Reynolds 1989).

Differential thermal analysis. DTA measurements were carried out using a Setaram model TG-DTA 92 instrument with alumina as reference. The sample was maintained in an inert atmosphere of N_2 throughout the heating period, and the temperature was increased at a linear rate of 8 C/min.

Chemical analyses of exchangeable cations. Hydrothermally treated Lu-saturated smectites were submitted to a further Lu-exchange process using a procedure similar to that employed to prepare the initial Lu-saturated samples. Concentrations of Al, Mg, and Fe in the extracts were determined by atomic absorption spectroscopy, and Li was determined in the extracts from the hectorite sample using flame emission spectroscopy.

RESULTS AND DISCUSSION

Differential reactivity of smectites

Figure 2 shows the XRD patterns obtained for the entire set of initial exchanged smectites, both in Lu^{3+} and in Na^{+} (top and bottom patterns of each plot, respectively). All the patterns are made up of two distinct types of reflections, general and basal, which have been indexed in Figure 1a for the case of the Trancos montmorillonite. The general reflections, also called *hk* bands, have been shadowed in Figure 1. They are composed of asymmetrical lines with the characteristic "saw-tooth" shape of the two-dimensional reflections (Warren 1941). Such reflections are caused by the structure of the smectite layers themselves, and are independent of external conditions. Therefore, the general nature of the *hk* band system is the same for all the smectites, and the differences are in the details of spacing and relative intensities. An exception is the 060 reflection for which marked differences are observed in both position and relative intensity for the dioctahedral and trioctahedral smectites. Trioctahedral samples (Figs. 2c and 2d) show larger spacings and higher intensities (almost equal to the 11/02 reflection), in agreement with literature data (e.g., Grim 1968).

The basal reflections, on the other hand, have symmetrical peaks whose positions vary with the separation between the layers. This separation depends on the nature of the cations present in the interlayer space, the *b*-dimension of the smectite unit cell, the amount of water, and the chemical reactions to which the mineral may have been subjected. Thus, Na-saturated smectites show two different basal spacings depending on the octahedral character of the sample and, therefore, on the *b*-dimension of the lattice. Samples with higher values of *b* (the trioctahedral ones) exhibit lower basal spacings (Davidtz and Low 1970). However, all the Lu-exchanged smectites show the same basal spacing value of 15.3 Å, independent of the *b*-dimension, in agreement with previous data reported for smectites saturated with multivalent cations (Ravina and Low 1977).

XRD patterns for the Lu-smectites subjected to hydrothermal treatment at 150 atm and 400 C for 24 hours are shown in Figure 3. Smectite reflections are the only ones present in the patterns for both the Arizona montmorillonite and the hectorite (Figs. 3b and 3d, respectively). However, the patterns for the Trancos montmorillonite (Fig. 3a) and the saponite (Fig. 3c)

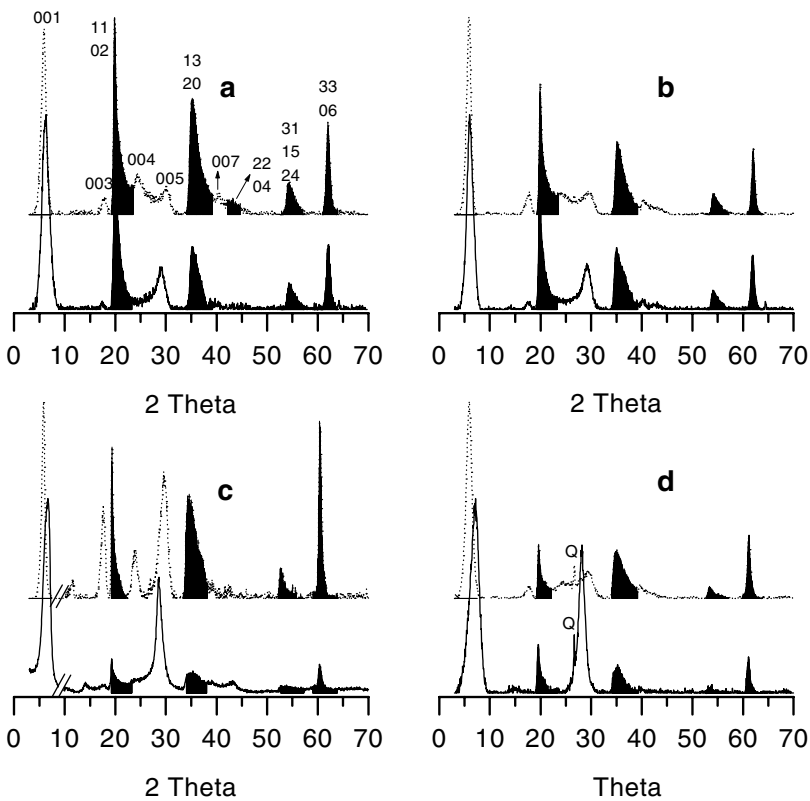

FIGURE 2. X-ray diffraction patterns of the untreated Na-saturated (solid lines) and Lu-saturated (dotted lines) smectites. **(a)** Trancos montmorillonite. **(b)** Arizona montmorillonite. **(c)** Saponite. **(d)** Hectorite. *hk* bands shaded.

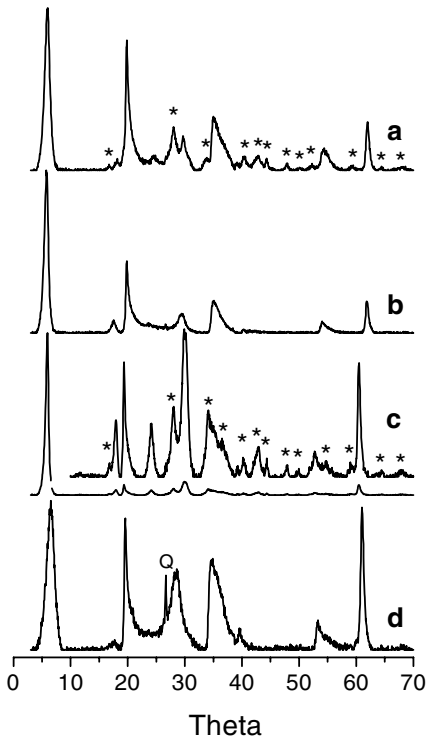

FIGURE 3. X-ray diffraction patterns of the Lu-saturated smectites hydrothermally treated at 400 C and 150 atm for 24 hours. **(a)** Trancos montmorillonite. **(b)** Arizona montmorillonite. **(c)** Saponite. **(d)** hectorite. * = reflections corresponding to the $Lu_2Si_2O_7$ phase. Q = quartz.

show several additional new reflections (marked with asterisks), which are consistent with the development of the crystalline phase $Lu_2Si_2O_7$ (JCPDS file number 34-0509). Thus two different degrees of reactivity in the formation of the new $Lu_2Si_2O_7$ phase are deduced, which depend on the presence of tetrahedral Al.

A comparison between Figures 3a and 3c shows that, although both of them include a similar number of reflections corresponding to $Lu_2Si_2O_7$, the intensity ratio of the peaks corresponding to the disilicate and the smectite phases are larger for the saponite sample. To clarify this point, the saponite diagram was drawn in Figure 3c using a scale in which the 11 and 02 *hk* general reflection for the smectite phase, appearing at 20 2θ, have heights similar to those of the same reflection in the Trancos montmorillonite diagram (Fig. 3a). At this scale, the general enhancement of the disilicate reflections is clearer in the saponite. In particular, the ratio of the main reflection of $Lu_2Si_2O_7$ at 28 2θ to that of the main general reflection of the smectite at 20 2θ is almost double in saponite than in Trancos montmorillonite. Therefore, the existence of tetrahedral Al in the smectite layer seems to be the first structural aspect that enhances the reactivity of the smectite group for the formation of the disilicate phase. This fact can be explained in terms of the higher electrostatic attraction between the interlayer Lu ions and the tetrahedral sheet in tetrahedrally substituted samples than in smectites without this kind of substitution. The more localized character of the negative charge in the vicinity of the Al tetrahedra (Sposito and Prost 1982) can account for this experimental result.

To determine the effect, if any, of the other structural parameters on the reactivity of the smectites, XRD patterns were

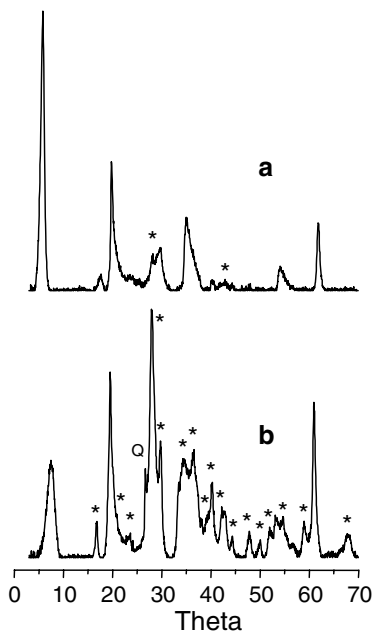

FIGURE 4. X-ray diffraction diagrams of **(a)** Arizona Lu-montmorillonite and **(b)** Lu-hectorite hydrothermally treated at 400 C and 200 atm for 24 hours. * = reflections corresponding to the $Lu_2Si_2O_7$ phase. Q = quartz.

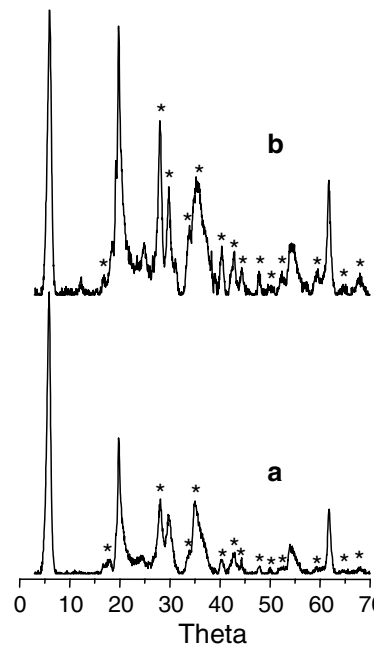

FIGURE 5. X-ray diffraction patterns of Arizona Lu-montmorillonite hydrothermally treated at 400 C for 24 hours at **(a)** 250 atm and **(b)** 300 atm. * = reflections corresponding to the the $Lu_2Si_2O_7$ phase.

recorded at increased pressures for the less-reactive minerals, i.e., those without tetrahedral Al. Figure 4 illustrates the diffraction patterns for the Arizona montmorillonite and the hectorite treated hydrothermally at 200 atm and 400 C for 24 hours. The XRD patterns reveal the presence of disilicate reflections, marked with asterisks, for both smectites. However, whereas a complete set of reflections corresponding to the disilicate phase is observed in the hectorite, the Arizona montmorillonite pattern exhibits only two new peaks. Consequently, the second structural factor that seems to modulate the hydrothermal reactivity of the smectite for the formation of $Lu_2Si_2O_7$ is octahedral occupancy; i.e., trioctahedral sheets are more reactive. This secondary effect is shown by those samples without tetrahedral Al, hectorite being more reactive than Arizona montmorillonite, as well as by those with tetrahedral Al, saponite being the most reactive. In the latter case, the tetrahedral Al content is higher in the saponite. Both structural parameters make saponite the most reactive candidate for the studied reaction.

To fulfill the first objective of this study—to determine whether the formation of $Lu_2Si_2O_7$ was a general reaction for the smectite group—further experiments were carried out at higher pressures on the least-reactive sample, the Arizona montmorillonite. These experiments indicate that this sample has similar XRD patterns to those observed for the other smectites (Fig. 5) when it is subjected to higher pressures (250 and 300 atm). This finding leads to the conclusion that the formation of $Lu_2Si_2O_7$ is a general outcome for the Lu-saturated members of the smectite group, although different pressures are needed for its complete development.

As regards the last structural parameter analyzed, the layer charge, the results obtained here do not indicate any relation-

most reactive samples (saponite and Trancos montmorillonite), exhibit intermediate layer-charge values, and the samples having maximum and minimum layer charge values are the group of less-reactive ones. Consequently, the layer charge, within the smectite range, does not have observable effects on hydrothermal reactivity.

The ability of Lu^{3+} situated in the interlayer space to alter the reactivity of these minerals in comparison with samples saturated with other cations, e.g. Na^+, is illustrated in Figure 6. This diagram displays the XRD patterns for the Lu- and Na- smectite samples hydrothermally treated at 400 C for 24 hours at a pressure as high as 250 atm. Lu-smectite diagrams (dashed lines) show, in all cases, the whole set of $Lu_2Si_2O_7$ reflections along with those for smectite. However, Na-smectite patterns show only those reflections corresponding to the smectite phase.

Residual structure of the smectites

The formation of $Lu_2Si_2O_7$ from Lu-saturated smectites should produce at least two types of changes in the structure of the layered silicates. First, after hydrothermal treatment, exchangeable Lu^{3+} ions form a new crystalline phase and no longer occupy interlayer positions. Second, Si^{4+} ions of the new disilicate phase have left their structural locations in the tetrahedral sheet of the smectites. The study of these modifications and the determination of the residual structure of the smectites are of fundamental importance. On the one hand, they are related to basic aspects of layer-silicate chemistry, such as the leaching of structural cations (Komadel 1996; Corma 1987) and the diffusion of metal ions through lattice positions (Rhodes 1995; MacKenzie 1996). On the other hand, a precise knowledge of the reactivity of these systems for further treatments is

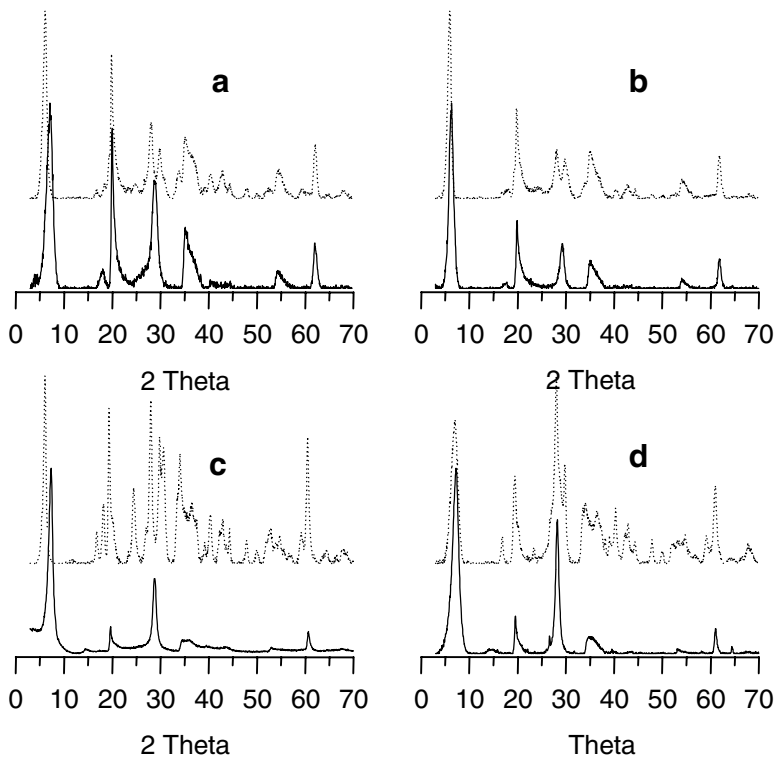

FIGURE 6. X-ray diffraction patterns of the Na-saturated (solid lines) and Lu-saturated (dotted lines) smectites hydrothermally treated at 400 C and 250 atm for 24 hours. **(a)** Trancos montmorillonite. **(b)** Arizona montmorillonite. **(c)** Saponite. **(d)** Hectorite.

necessary to determine their usefulness as active materials in the different processes for which they are proposed.

Because these changes essentially alter the short-range order of the constituent elements of the smectites, experimental techniques are required that examine the local atomic environments. We will report the results of a multinuclear, solid-state nuclear magnetic resonance (MAS-NMR) study of these smectites in a separate contribution. In this paper, we report an XRD analysis, including diffractograms from oriented aggregates, as well as DTA measurements and determination of the exchangeable cations after hydrothermal treatments, providing useful information on the residual structure of the minerals.

XRD study. A re-examination of the XRD patterns obtained for the Lu-saturated smectites after the hydrothermal treatments (Fig. 3–6) enables two observations. First, the hydrothermal treatments do not affect the general *hk* reflections of the smectites, which remain at the same positions and with the same shape as in the initial samples. However, in some cases, mainly in the diffractograms corresponding to the more severely treated smectites, the curves are modified near these *hk* reflections due to the appearance of reflections corresponding to the new crystalline phase. This result confirms the permanence of the general sheet structure of these layered materials after the hydrothermal reaction even in the case of the more intense treatments. It should be pointed out that only ~4% of the total number of Si atoms present in the system are required to transform all the available Lu ions into the disilicate phase. Consequently, it should not be surprising that an extensive amount of the new crystalline phase co-exists with a large portion of the remaining smectite phase.

On the other hand, all the smectites analyzed after the hydrothermal treatments exhibit basal reflections with spacings compatible with expanded layers. This result means that some interlayer species are present and cause this interlayer separation. Because the Lu ions form part of a new crystalline structure, the new interlayer space should be occupied either by hydrated cations that diffused there through the lattice, or by more rigid structures—cross-linked polyoxocations—formed during the hydrothermal reaction. To resolve this question, oriented aggregates were prepared in water and in ethylene glycol (EG) for the initial samples and those treated hydrothermally at 250 atm. The basal spacings of those samples obtained from the first basal reflection position have been plotted in a histogram (Fig. 7). The striped bars indicate the aggregates in EG. All the samples, before and after the hydrothermal treatment, show a basal spacing of 17 Å, corresponding to a two-layer complex of EG. This behavior is typical of layered silicates with a wide range of interlayer cations of all valences (Brown 1961). Thus, the hypothesis of the existence of rigid structures in the interlayer space is ruled out, and the idea of cation diffusion from the lattice is supported. The solid gray bars represent the basal spacings obtained from the aggregates in water, which will provide some information for the identification of cations diffusing to the interlayer space. All the initial samples exhibit the same d_{001} value of 15.3 Å, compatible with a Lu aqueous complex in the interlayer region of the smectite, as previously reported by us (Muñoz-Páez et al. 1994). However, the hydrothermal treatment causes different basal spacings: the dioctahedral smectites (Arizona and Trancos montmorillonite) show the same d_{001} as observed for the initial samples; saponite experiences a slight basal contraction, with a basal spacing of 14.8 Å compatible with a two-layer hydrate; and the d_{001} value of hectorite diminishes markedly to 12.6 Å, corresponding to a mono-hydrate state.

The smectite basal spacing depends on the water-vapor pressure under which the sample has been prepared, on the particular smectite group mineral analyzed, and on the exchangeable cation present in the interlayer space. As all the XRD measurements were carried out at the same humidity, the only factors determining basal spacing should be the mineral and the interlayer cations. As regards the former, all the smectites with the same *b*-dimension should exhibit similar swelling behavior, as reported in the previous section (Davidtz and Low 1970). This fact transforms the dioctahedral smectites into low-sensitivity samples for this experiment, as their basal spacings when saturated with either Lu^{3+} or Na^{+} are very similar. With regard to the second factor, the cations that may have diffused to the interlayer space of each smectite is determined by both the amount and the type of the cations initially located in the structural positions of the lattice. It is generally accepted in investigations of leached aluminosilicates that: (1) ions in the tetrahedral sheet are more difficult to leach than those located in the octahedral one (Breen 1995; Kaviratna 1994), and (2) smectites with high Mg contents in the octahedral layer are leached more readily than those containing a higher proportion of Al. In particular, the rate of ion leaching observed here decreases in the order $Li^{+} > Mg^{2+} > Fe^{3+} > Al^{3+}$, in accordance with previous workers (Corma 1987; Komadel 1996). Bearing this series in mind, along with the composition and the d_{001} value of the smectites analyzed here, the following comments can be made.

(1) Hectorite suffers the more drastic change in its basal spacing and it is the only smectite containing octahedral Li.

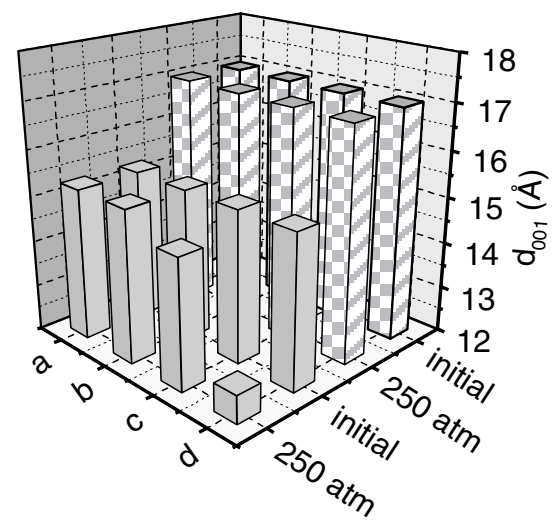

FIGURE 7. Histogram showing the basal spacing values obtained from the oriented aggregates in ethylene glycol (stripped bars) and water (solid-gray bars) of the initial and hydrothermally treated at 250 atm Lu-smectites. **(a)** Trancos montmorillonite. (b) Arizona montmorillonite. **(c)** Saponite. **(d)** Hectorite.

These ions should have diffused, partially or totally, to interlayer positions during the hydrothermal treatment, and should be responsible for the observed low d_{001} values.

(2) Saponite, which contains a large proportion of Mg^{2+} ions in the octahedral sheet, shows a slightly reduced d_{001} value that is compatible with a two-hydrate state. This situation should be due to the diffusion of Mg^{2+} ions to the interlayer space.

(3) The less-sensitive XRD response of the montmorillonite samples to the nature of the cations located in the interlayer space does not allow us to infer which cations have been leached during the hydrothermal treatment. To identify these cations, as well as to corroborate the previous assessments, DTA measurements and chemical analyses of the exchangeable cations have been performed.

Thermal analyses. DTA curves for the four Lu-saturated smectites before (solid lines) and after (dotted lines) hydrothermal treatments at 250 atm are plotted in Figure 8 for the 0-300 C temperature range. In that range, DTA curves show endothermic reactions due to the loss of molecular water, present mostly in interlayer sites. The amount of this water depends on the nature of the interlayer cations, the pretreatment of the sample, and the nature of the silicate lattice (Grim 1968). Two types of water molecules can be distinguished in the interlayer space of the smectites: filling water, which belongs to outer hydration shells of the cations or is bound to the oxygen surface of the smectite sheets; and water belonging to the first shell of hydration of the exchangeable cations. Because the initial Lu-saturated smectites have both the same pre-treatment and the same interlayer cation, the differences observed in the curves (solid lines) can be attributed only to changes in the hydration of the silicate surfaces. Vertical lines labeled with the corresponding temperature values have been included for the DTA curves of the initial samples at the positions where the endothermic peaks are observed. These temperatures, ranging from 118 C in the hectorite to 140 C in the Arizona montmorillonite, are in good agreement with the layer charge deficits of the smectites: the larger the layer charge, the higher the dehydration temperature. Moreover, samples with a higher layer charge exhibit a wider endothermic peak and an enhancement of the shoulder appearing on its right wing (second dehydration peak) associated with the more tightly bonded water molecules.

The DTA curves for the samples after hydrothermal treatment (dotted lines in Fig. 8) are modified in three aspects:

(1) All the DTA curves show minima at slightly lower temperatures than those observed for the initial samples. This shift may be due to both a decrease in the layer charge deficit of the silicate and the incorporation of new cations in the interlayer space with lower hydration energies.

(2) The DTA curve for hectorite (Fig. 8d) exhibits a second dehydration reaction centered at 170 C, which resembles DTA curves reported in the literature for Li-saturated hectorites (Greene-Kelly 1952). Consequently, both the XRD patterns from the water aggregates and these DTA measurements indicate a diffusion of Li ions to the interlayer space in this sample.

(3) The other samples yield similar DTA curves composed of three overlapping components marked with arrows in Figures 8a–8c. A study of DTA curves reported in the literature for exchanged-smectite derivatives (El-Barawy et al. 1986), together with considerations of the lattice compositions of the smectites analyzed here, indicate that Mg^{2+} ions have been leached from the octahedral sheets. In Mg-exchanged smectites, the high enthalpy of the last dehydration reaction (at around 225 C) was interpreted by Koster van Groos and Guggenheim (1987) as due to the release of water molecules tightly bonded to the structure. This bonding can be explained by the interaction between the dipole of the water molecules and the Mg cations at one end and the charge-undersaturated basal oxygen atoms associated with Al-substituted tetrahedra at the other. To

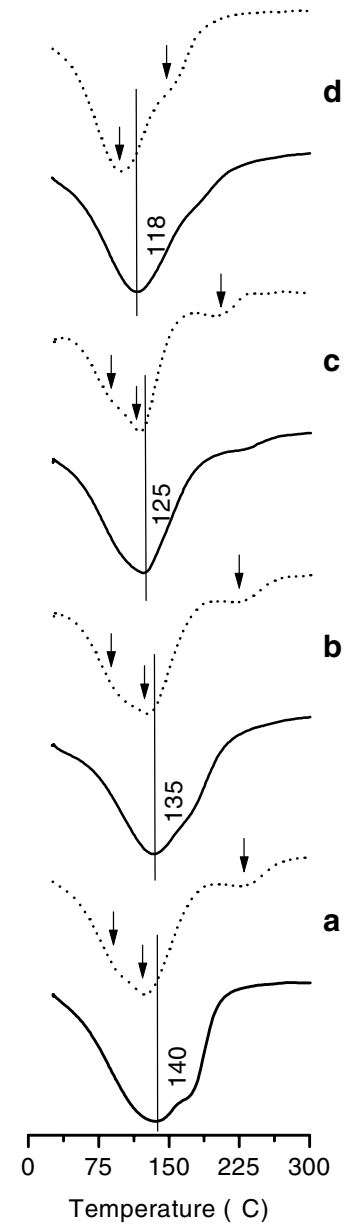

FIGURE 8. DTA diagrams of the four Lu-smectites untreated (solid line) and hydrothermally treated at 400 C and 250 atm for 24 hours (dashed line). **(a)** Arizona montmorillonite. **(b)** Trancos montmorillonite. **(c)** Saponite. **(d)** Hectorite. Arrows as described in the text. All are plotted on the same scale.

fulfill these two requirements, Mg ions must be present in the interlayer space and Si must be substituted by Al in the tetrahedral sheet. The diffusion of octahedral Al to vacant tetrahedral positions should be necessary for those initial smectites without tetrahedral Al, apart from the leaching of Mg ions to the interlayer space. This point will be discussed in a subsequent MAS-NMR paper on these systems.

Analyses of the exchangeable cations. Table 2 shows the amounts of Li, Mg, Fe, and Al extracted from the Arizona Lu-montmorillonite, the Lu-saponite, and the Lu-hectorite after hydrothermal treatment and re-saturation with Lu ions. Due to the difficulties in comparing cation-exchange capacities in samples that have suffered considerable textural and structural changes during the hydrothermal treatments, only a qualitative discussion of the analyses will be included.

Lithium and Mg are leached from the octahedral sheet of the Lu-saturated hectorite as $Lu_2Si_2O_7$ is formed. The absence of the third dehydration reaction in its DTA curve, even when Mg ions are present in the interlayer space, can be explained by the absence of structural Al in the hectorite sample, which prevents the diffusion of these ions to tetrahedral positions during the treatment. The two other samples, the Arizona montmorillonite and the saponite, only suffer leaching of Mg ions.

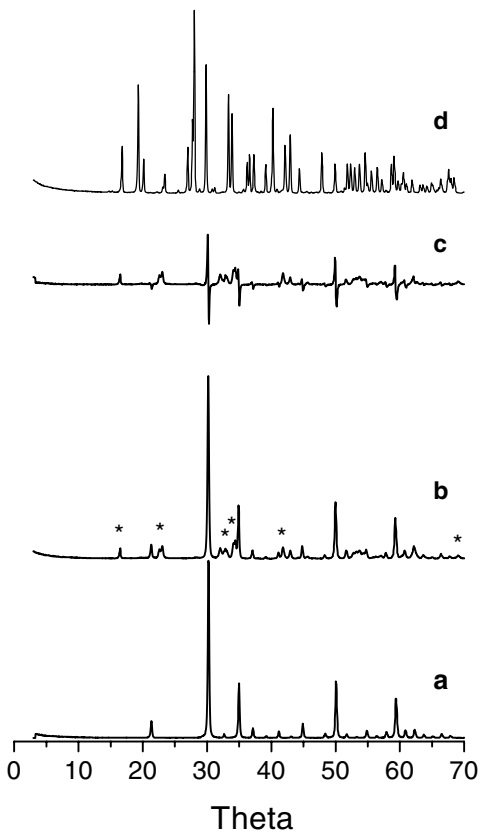

FIGURE 9. X-ray diffraction patterns of **(a)** the initial $2SiO_2$:$1Lu_2O_3$ mixture **(b)** the product obtained after hydrothermal treatment of the mixture at 400 C and 24 hours at 250 atm (* = new reflections) **(c)** plot b-plot a and **(d)** the product obtained after thermal treatment of the mixture at 1500 C for 24 hours in air.

This leaching is determined in the case of the saponite by the octahedral composition, Mg^{2+} being the most abundant cation in those positions. However, it indicates a higher leaching rate for this cation, compared with Fe or Al ions, from the montmorillonite. This leaching order is compatible with results previously reported in the literature (Corma 1987).

Differential reactivity for framework and sheet silicates

A last set of experiments, using thermally and hydrothermally treated Lu_2O_3-SiO_2 mixtures, was carried out to study this system and compare it with the reactivity shown by the smectites in the formation of the $Lu_2Si_2O_7$. Figure 9 shows the XRD patterns obtained for the starting mixture of oxides (Fig. 9a), after heating for 24 hours at 400 C and 250 atmospheres (Fig. 9b), and after heating at 1500 C for 24 hours in air (Fig. 9d). The hydrothermal treatment is the same as that employed to obtain all the $Lu_2Si_2O_7$ reflections from the Lu-saturated smectites, and the thermal treatment is that previously reported to obtain $Lu_2Si_2O_7$ from the mixture of oxides (Felsche 1973).

The XRD pattern for the initial mixture of oxides shows all the reflections indexed for the cubic form of Lu_2O_3 (JCPDS file number 12-0278). Due to the non-crystalline state of the silica employed, there is no reflection corresponding to this oxide. Not even the wide band characteristic of amorphous silica at ~21 2θ is observable in the pattern because of the low intensity of this band compared with the Lu_2O_3 reflections.

The XRD pattern following hydrothermal heating at 400 C includes all the former reflections corresponding to the Lu_2O_3, together with a half dozen weak reflections that have been marked in Figure 9b with asterisks. Consequently, a low reactivity of the system under these experimental conditions is inferred. To determine which incipient phase is appearing, a subtraction of the XRD patterns corresponding to the initial and the hydrothermally treated mixture of oxides was performed (Fig. 9c), which reveals the set of new reflections mentioned above (along with spurious features at 30 , 35 , 50 , and 59 2θ arising from imperfect subtractions). These reflections can be compared with those of $Lu_2Si_2O_7$ appearing from the oxide mixture heated at 1500 C (Fig. 9d). It is clear that there is no relationship between the two patterns and, thus, there is no evidence for formation of $Lu_2Si_2O_7$ after hydrothermal treatment of the mixture of oxides.

SUMMARY

The results reported here allow the following conclusions to be drawn regarding the enhanced hydrothermal reactivity of Lu-saturated smectites to form $Lu_2Si_2O_7$.

(1) $Lu_2Si_2O_7$ forms at temperatures as low as 400 C under hydrothermal conditions from Lu-saturated smectites, the pro-

TABLE 2. Amounts of Li, Mg, Fe, and Al, expressed in meq/100 g, determined from the extracts obtained during the ionic exchange process of the Lu-smectites hydrothermally treated at 400 C during 24 hours and 250 atm

Sample	Li	Mg	Fe	Al
Hectorite	46.9	47.8	n/d	n/d
Saponite	–	75.8	n/d	n/d
Arizona montmorillonite	–	62.4	n/d	n/d

n/d = not detected.

cess being possible for all the smectite samples analyzed. This enhanced reactivity appears to be caused mainly by the crystal structure of smectites, rather than by the experimental hydrothermal conditions employed, as the same treatment does not induce similar changes in Lu_2O_3-SiO_2 mixtures. The proximity between the elements involved in the reaction as well as the high mobility of the hydrated cations in the interlayer space of hydrothermally treated smectites are the basic structural characteristics of the smectites responsible for the lowering of the activation energy of the process.

(2) The existence of tetrahedral substitutions in the smectites also enhances reactivity. Therefore, the initiation of the reaction from interactions between interlayer Lu^{3+} cations and Si atoms surrounded by tetrahedral Al atoms should be more favored than from interactions between interlayer Lu^{3+} cations and Si atoms surrounded by another three tetrahedral Si atoms. The more-localized character of the negative charge in the vicinity of the Al tetrahedra should cause a higher electrostatic attraction between these ions and the interlayer Lu ions (Sposito and Prost 1982) and, consequently, it should confer a higher reactivity on these Si atoms.

(3) The reactivity of the trioctahedral smectites is enhanced slightly compared with dioctahedral types. This structural parameter affects the leaching process occurring simultaneously with the formation of $Lu_2Si_2O_7$. Two structural aspects of the trioctahedral series should be responsible for the more favorable progress of the reaction. First, octahedral ^{VI}M-O bonds are required to break to release SiO_4 tetrahedra from the shared (octahedral-tetrahedral) oxygen layer. From simple electrostatic considerations, the trioctahedral ^{VI}M-O bonds, involving Li^+ and Mg^{2+} cations, will be broken more easily than the dioctahedral ones. Second, the migration of the initial interlayer Lu ions requires the incorporation of new cations in these positions. The leaching rate associated to the octahedral cations, Li^+ and Mg^{2+}, appearing in the trioctahedral series are higher than those associated with the cations mostly appearing in the dioctahedral series.

(4) The system formed by Lu-saturated smectites is more reactive than that formed by a mixture of oxides; the hydrothermal conditions employed are successful for the formation of the $Lu_2Si_2O_7$ only in the former case. The close proximity of the reactant elements, Lu and Si, should, therefore, be the main structural parameter enhancing the observed reactivity in the group of the smectites.

ACKNOWLDGEMENTS

We gratefully acknowledge the financial support from the DGICYT (Project no. PB97-0715) and one of us (A.I.B.) thanks the Spanish M.E.C. for a predoctoral fellowship which has allowed carrying out the experimental work included in this report.

REFERENCES CITED

Alba, M.D., Alvero, R., Becerro, A.I., Castro, M.A., Muñoz-Páez, A., and Trillo, J.M. (1996) Formation of High-Temperature Lutetium Disilicate from Lutetium-Saturated Aluminosilicates in Mild Conditions. Incorporation of Si and Al XAS Techniques to the Study of These Systems. Journal of Physical Chemistry, 100, 19559–19567.

Alba, M.D., Alvero, R., Becerro, A.I., Castro, M.A., Muñoz-Páez, A., and Trillo, J.M. (1997) Study of the reversibility of the local La^{3+} environment after thermal and drying treatments in lanthanum-exchanged smectites. Nuclear Instruments and Methods in Physics Research B, 133, 34–38.

Alvero, R., Alba, M.D., Castro, M.A., and Trillo, J.M. (1994) Reversible Migration of Lithium in Montmorillonites. Journal of Physical Chemistry, 98, 7848–7853.

Ames, L.L., Sand, L.B., and Goldich, S.S. (1958) A contribution on the Hector, California, bentonite deposit. Economic Geology, 53, 22–37.

Association International Pour l´Etude des Argiles Nomenclature Committee (1980) Summary of recommendations of AIPEA nomenclature committee. Clays and Clay Minerals, 28, 73–78.

Beall, G.W., Ketelle, B.H., Haire, R.G., and O'Kelley, G.D. (1979) Radioactive Waste in Geological Storage. In S. Fried, Ed., ACS Symposium Series 100, p.201–213. American Chemical Society, Washington, D.C.

Becerro, A.I. (1997) Desarrollo de un sistema modelo de análisis estructural de la reactividad química de compuestos de silicio 2D y 3D aplicado a la formación de $Lu_2Si_2O_7$. Ph.D. dissertation, Univeristy of Seville, Seville.

Breen, C., Madejová, J., and Komadel, P. (1995) Characterisation of moderately acid-treated, size-fractionated montmorillonites using IR and MAS NMR spectroscopy and thermal analysis. Journal of Materials Chemistry, 5, 469–474.

Brown, G. (1961) The X-Ray Identification and Crystal Structure of Clay Minerals. Mineralogical Society. Clay Minerals Group. London.

Castro, M.A., Alba, M.D., Alvero, R., Becerro, A.I., Muñoz-Páez, A., and Trillo, J.M. (1996) Formation at 300 C of a high temperature disilicate from hydrated lutetium in a layered aluminosilicate. Clay Minerals, 31, 507–512.

Corma, A., Mifsud, A., and Sanz, E. (1987) Influence of the chemical-composition and textural characteristics of Palygorskite on the acid leaching of octahedral cations. Clay Minerals, 22, 225–232.

Davidtz, J.C. and Low P.F. (1970) Relation between crystal-lattice configuration and swelling of montmorillonites. Clays and Clay Minerals, 18, 325–332.

El-Barawy, K.A., Girgis, B.S., and Felix, N.S. (1986) Thermal treatment of some pure smectites. Thermochimica Acta, 98, 181–189.

Felsche, J. (1973) The Crystal Chemistry of Rare-Earth Silicates. Structure and Bonding, 13, 99–495.

Figueras, F. (1988) Pillared Clays as Catalysts. Catalysis Review-Science and Engineering, 30, 457–499.

Greene-Kelly, R. (1952) Irreversible dehydration in montmorillonite. Clay Minerals Bulletin, 1, 121–227.

Grim, R.E. (1968) Clay Mineralogy: McGraw-Hill Book Company, New York.

Kaviratna, H. and Pinnavaia, T.J. (1994) Acid hydrolysis of octahedral Mg^{2+} sites in 2:1 layered silicates: an assessment of edge attack and gallery access mechanisms. Clays and Clay Minerals, 42, 717–723.

Komadel, P., Madejová, J., Janek, M., Gates, W.P., Kirkpatrick, R.J., and Stucki, J.W. (1996) Dissolution of hectorite in inorganic acids. Clays and Clay Minerals, 44, 228–236.

Koster van Gross, A.F. and Guggenheim, S. (1987) Dehydration of a Ca- and a Mg-exchanged montmorillonite (Swy-1) at elevated pressures. American Mineralogist, 72, 292–298.

Mackenzie, K.J.D., Meinhold, R.H., Chakravorty, A.K., and Dafadar, M.H. (1996) Thermal reactions of alkali-leached aluminosilicates studied by XRD and solid-state ^{27}Al, ^{29}Si, and ^{23}Na MAS NMR. Journal of Materials Chemistry, 6, 833–841.

Miller, S.E., Heath, G.R., and González, R.D. (1982) Effects of Temperature on the Sorption of Lanthanides by Montmorillonites. Clays and Clay Minerals, 30, 111–122.

Moore, D.M and Reynolds, R.C. (Eds) (1989) X-ray diffraction and the Identification of Clay Minerals. Oxford University Press, Oxford, U.K.

Muñoz-Páez, A., Alba, M.D., Alvero, R., Castro, M.A., and Trillo, J.M. (1994) Geometric Structures of Lanthanide Ions within Layered Clays as Determined by EXAFS: From the Lu(III) Hydrate to the Disilicate. Journal of Physical Chemistry, 98, 9850–9860.

Muñoz-Páez, A., Alba, M.D., Alvero, R., Becerro, A.I., Castro, M.A., and Trillo, J.M. (1995) EXAFS study of the interaction of lanthanide cations with layered clays upon hydrothermal treatments. Nuclear Instruments and Methods in Physics Research B, 97, 142–144.

Ravina, I. and Low, P.F. (1977) Change of *b*-dimension with swelling of montmorillonite. Clays and Clay Minerals, 25, 201–204.

Rhodes, C.N. and Brown, D.R. (1995) Autotransformation and aging of acid-treated montmorillonite catalysts: A solid state ^{27}Al NMR study. Journal of the Chemical Society, Faraday Transactions, 91, 1031–1035.

Sposito, G. and Prost, R. (1982) Structure of Water Adsorbed on Smectites. Chemical Review, 82, 553–573.

Trillo, J.M., Poyato, J., Tobías, M.M., and Castro, M.A. (1990) Sorption of Water Vapour by M-Montmorillonite (M=Na, Li, La). Clay Minerals, 25, 485–498.

Trillo, J.M., Alba, M.D., Castro, M.A., Muñoz, A., Poyato, J. and Tobias, M.M. (1992) Local Environment of Lanthanum Ions in Montmorillonites upon Heating. Clay Minerals, 27, 423–434.

Trillo, J.M., Alba, M.D., Alvero, R., Castro, M.A., Muñoz-Páez, A., and Poyato, J. (1994) Interaction of Multivalent Cations with Layered Clays. Generation of Lutetium Disilicate upon Hydrothermal Treatment of Lu-Montmorillonite. Inorganic Chemistry, 33, 3861–3862.

Van Olphen, H. and Fripiat, J.J. (Editors) (1979) Data Handbook for Clay Minerals and Other Non-Metallic Materials. Pergamon Press, New York.

Warren, B.E. (1941) X-ray diffraction by random layers. Physical Review, 59, 693–698.

MANUSCRIPT RECEIVED JUNE 18, 1999
MANUSCRIPT ACCEPTED SEPTEMBER 3, 2000
PAPER HANDLED BY MARK WELCH